EXTENDED DATA

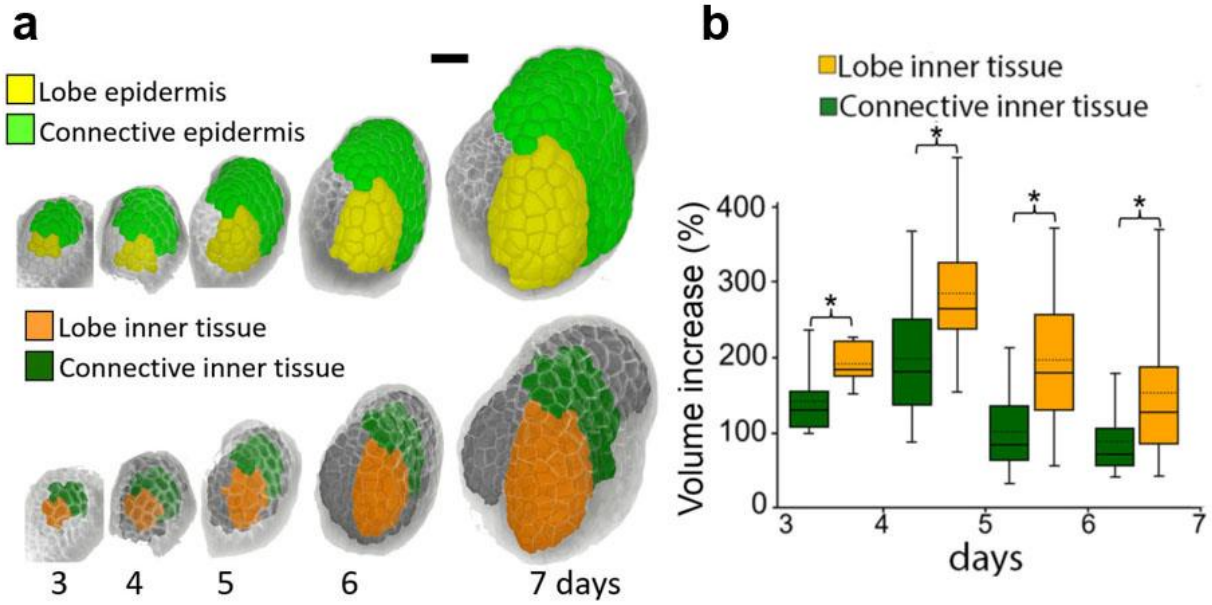

Extended Data Fig. 1 Localized growth in inner tissue underlies lobe formation. **a**, Lineage tracing of the anther regions, used for quantifications of growth shown. Colors indicate regions defined at the last time point traced back to the initial time point. **b**, Quantification of normalized volume increase per anther region in internal tissue (n>50 cells at each time point, 4 time-lapse series). Data was normalized by the mean growth in the connective region. Asterisks indicate statistical significance, Mann-Whitney U test, P<0.01. Scale bar, 20 µm.

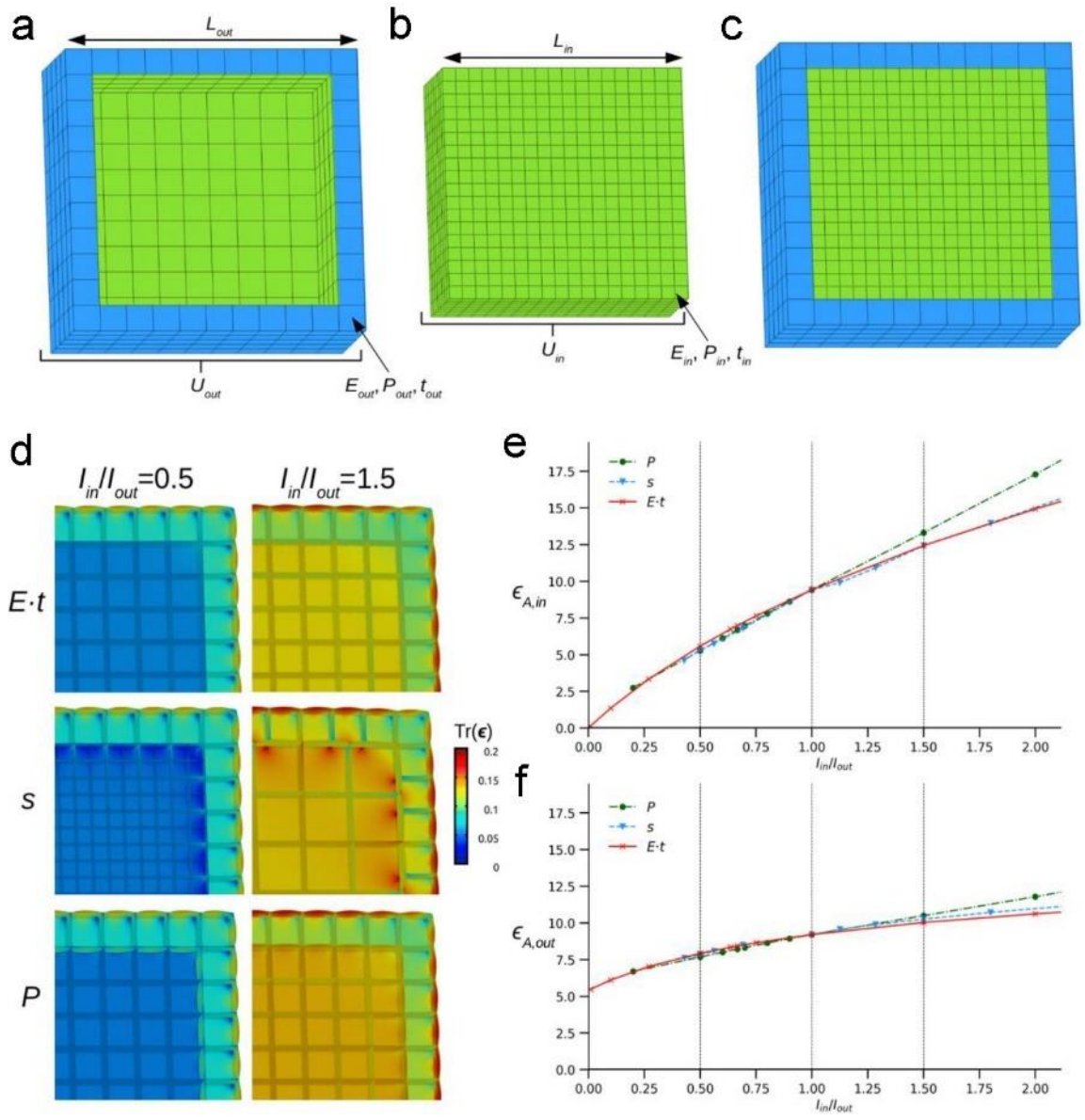

Extended Data Fig. 2 Cube of cube model details. a to **c,** Cross-section of the model template of the cube of cubes. **a**, Outer layer of the tissue with constant properties. It is of total size $L_{out}=U_{out}l_{out}$ where U_{out} is the number of cells along the side of the cubic tissue and l_{out} the side of those cells. **b,** Inner tissue of total size $L_{in}=(U_{out}-2)l_{out}$. It is made of U_{in}xU_{in}xU_{in} cells of size $l_{in}=L_{in}/U_{in}$. **c**, Assembled outer layer and inner tissue. **d,** Detailed view of Fig. 2B. The trace of the strain tensor is displayed as a heatmap. (**e** and **f**) For each parameter $E{\cdot}t$, s, and P, areal strains (in %) of anticlinal walls within inner **e** and outer **f** cells are plotted against the ratio of inflation potential in inner vs outer cells.

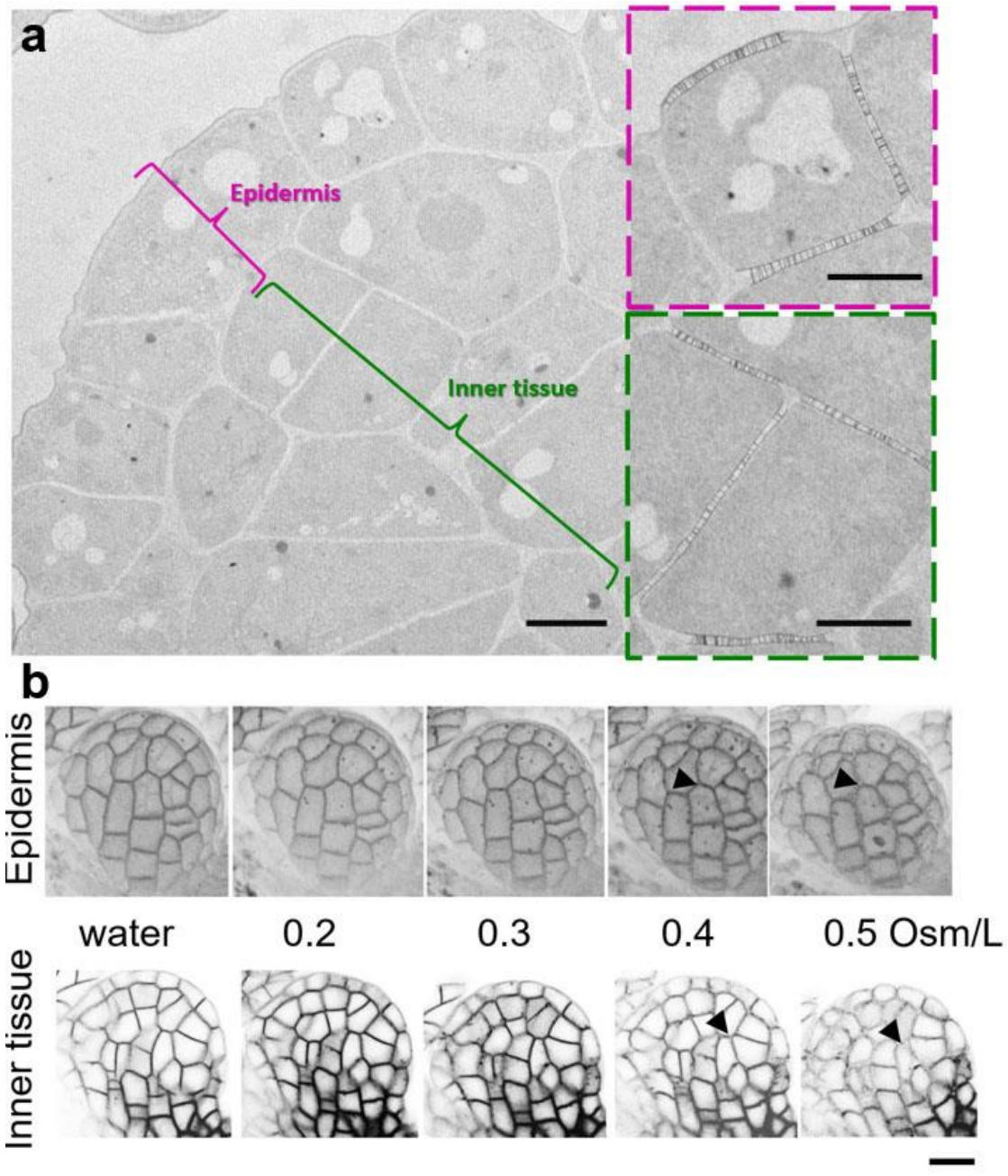

Extended Data Fig. 3 Measurements of cell wall thickness and Incipient plasmolysis analysis in ~4 days old anthers. **a,** Representative transmission electron microscopy micrograph of an anther lobe at a stage before lobation. Brackets indicate the layers considered for measurements as shown in Fig. 2e, epidermis (magenta) and inner tissue (green). Insets show segmented lines used to quantify cell wall thickness shown in Fig. 2f. **b**, Confocal images of anthers, before and after osmotic treatment with solutions of increasing NaCl concentration. The top row shows epidermis while the bottom row shows digital cross sections in the inner tissue. Arrow heads indicate the interstitial spaces created at incipient plasmolysis. Scale bars, 2.5 µm (a), 10 µm (b)

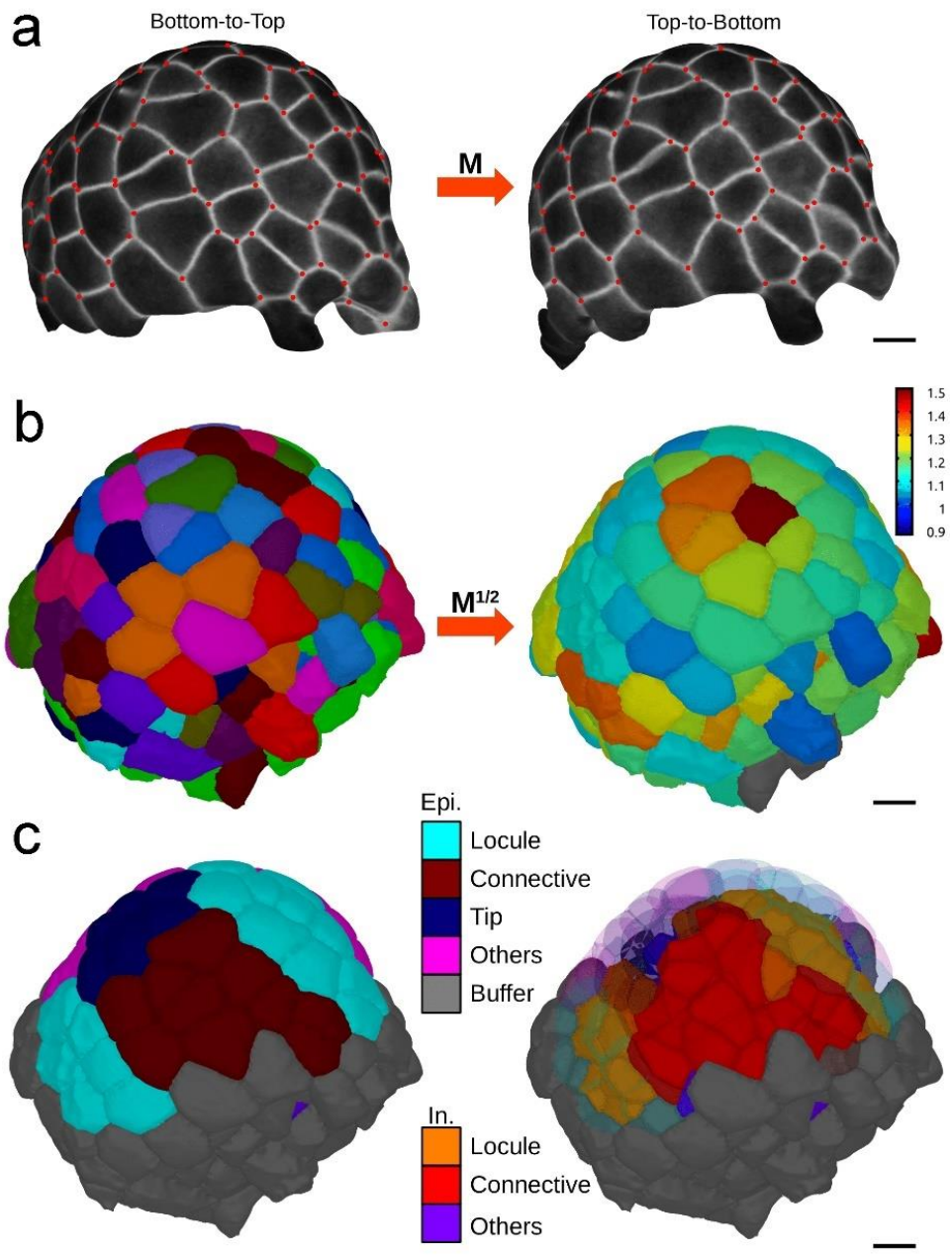

Extended Data Fig. 4 Obtaining the starting mesh for stiffness reverse-engineering. a, 2D meshes extracted from the top-to-bottom and bottom-to-top confocal microscopy scans of the same plasmolyzed sample Cell junctions are highlighted in red. We compute the transformation from one 3D point cloud to the other, M **b**, Starting mesh and transformed mesh obtained by applying half the transformation $M^{1/2}$ to the former. The heatmap of volume increase of each cell from the plasmolyzed experimental state to the turgid. **c**, Pooling of cells into regions. Regions are based on layer, connectivity and volume increase displayed in **b**. Scale bars, 5 µm.

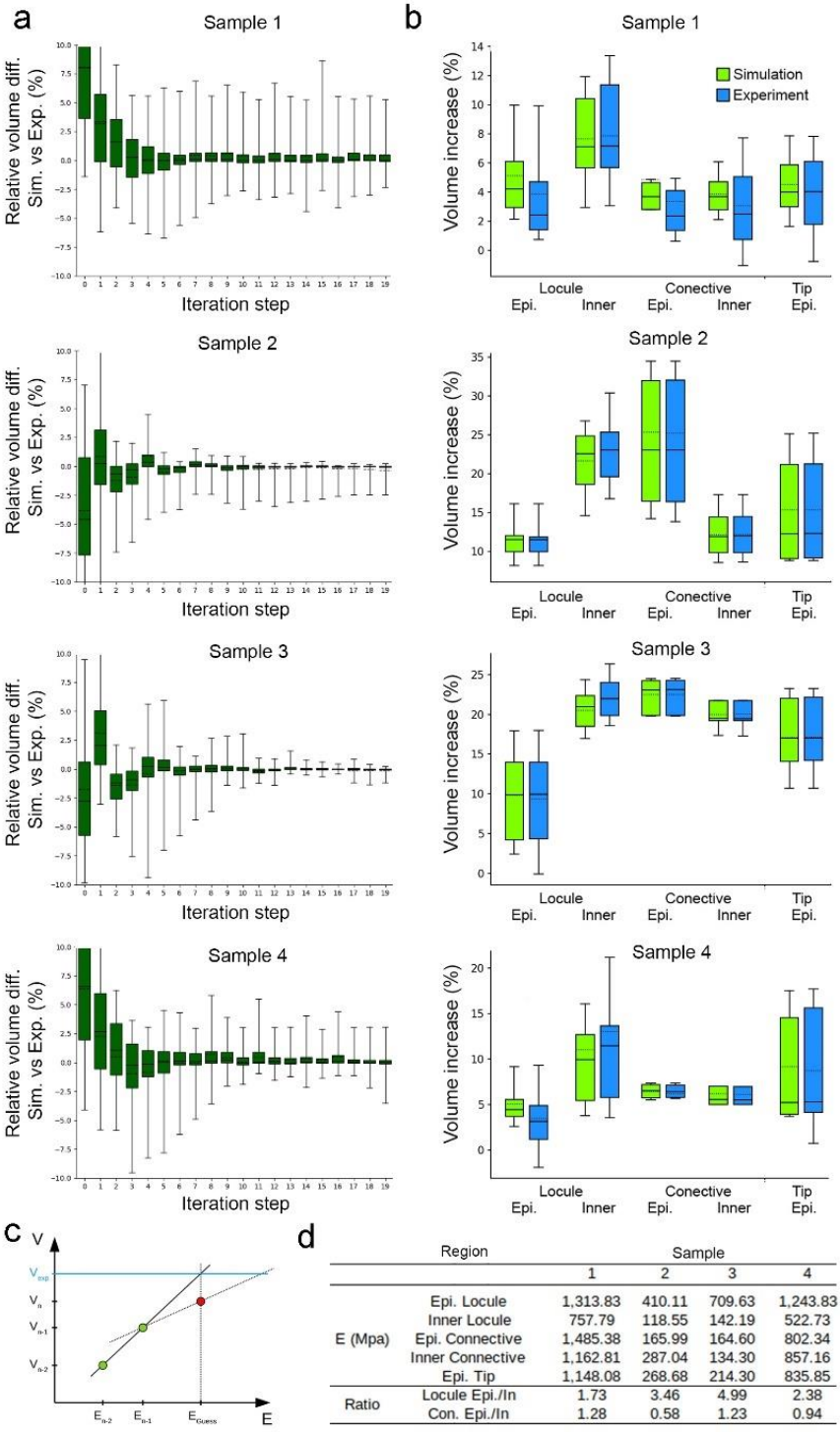

Region		Sample 1	Sample 2	Sample 3	Sample 4
E (Mpa)	Epi. Locule	1,313.83	410.11	709.63	1,243.83
	Inner Locule	757.79	118.55	142.19	522.73
	Epi. Connective	1,485.38	165.99	164.60	802.34
	Inner Connective	1,162.81	287.04	134.30	857.16
	Epi. Tip	1,148.08	268.68	214.30	835.85
Ratio	Locule Epi./In	1.73	3.46	4.99	2.38
	Con. Epi./In	1.28	0.58	1.23	0.94

Extended Data Fig. 5 Convergence of reverse engineering and significance of results. a, Convergence of the volume distribution of all cells of each sample over the reverse engineering steps. **b**, For each sample: final volume increase distributions from the plasmolyzed state to the turgid state, simulated and experimental. **c**, Guessing of the next stiffness of a given cell. A linear trend is drawn from the two previous states (E_{n-2},V_{n-2}) and (E_{n-1},V_{n-1}), and the intersection between this line and the V=V_{exp} horizontal line yields the new cell stiffness E_{Guess}. **d,** Stiffness values after the 20th reverse engineering step per region and stiffness ratios between regions of interest. An inner/outer gradient can be observed for each sample in the locule region.

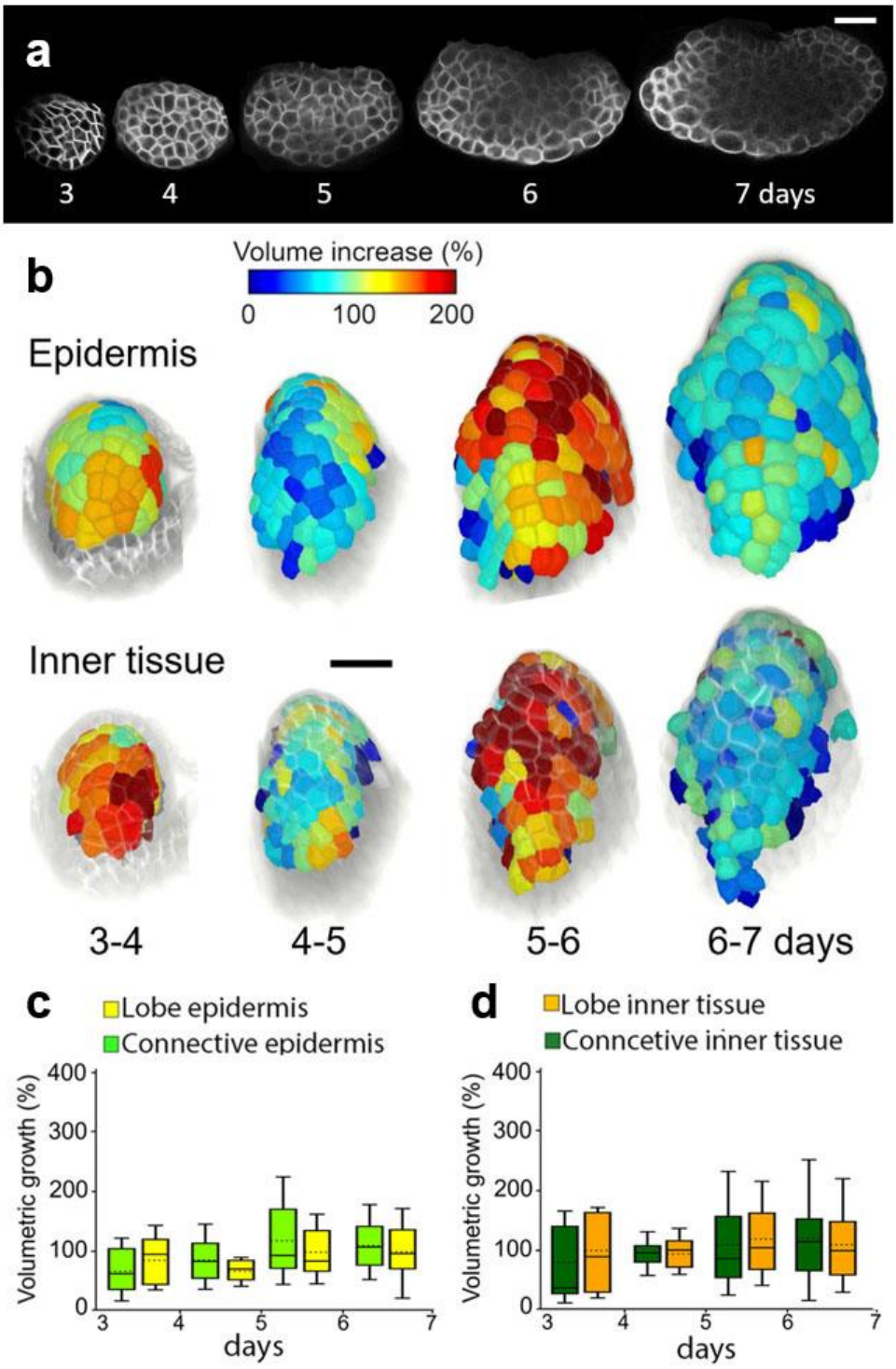

Extended Data Fig. 6 Lobe development is abolished in the absence of localized internal growth in the locule. **a**, Digital cross sections of a time-lapse series of the developing *spl-1* anther. **b,** Heat maps of volume increase in anther epidermis and inner tissue. **c** and **d,** Quantification of volume increase per anther region in the epidermis and inner tissue. No statistical significance, Mann-Whitney U test, $P<0.01$ ($n>50$ cells) was detected. Scale bars, 20 µm (a and b).

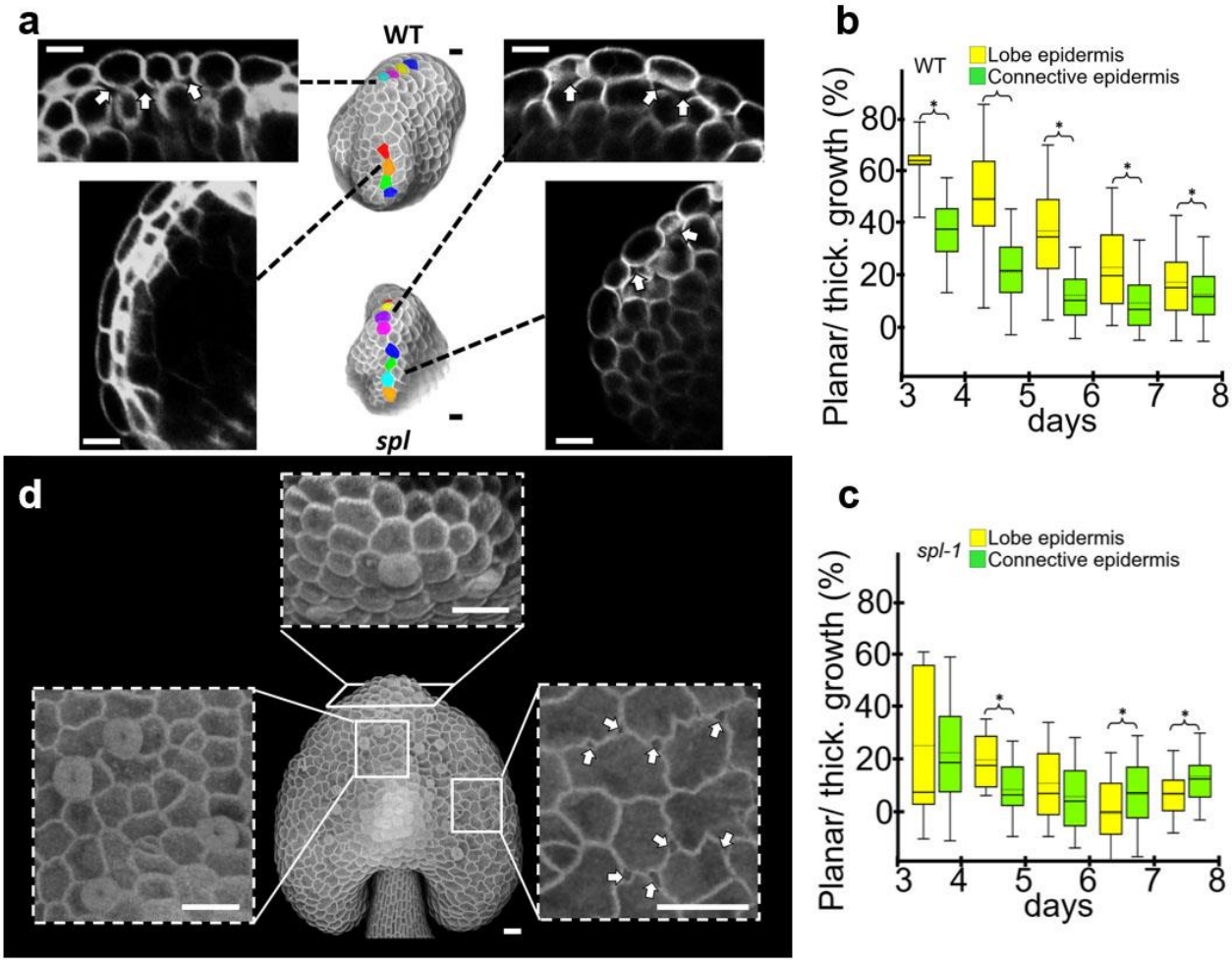

Extended Data Fig. 7 The epidermis in the anther lobe is under local tension **a,** Digital longitudinal cross sections of the anther lobe (top) and tip of connective (bottom) for wild type (left) and *spl/nzz* (right). Arrows indicate intercellular spaces. **b** and **c**, Quantification of ratio between cell growth within the organ plane and growth in cell thickness, per anther region in the epidermis in wild type **b,** and *spl-1* **c**,. Asterisks indicate statistical significance, Mann-Whitney U test, $P<0.01$ ($n>50$ cells). **d**, Confocal images of dissected *qua2-1* mutant anther. Insets show details of mid connective (left), tip of connective (top), and lobe (right). Arrows indicate points of cell detachments in the epidermis. Scale bars, 10 µm (a) 20 µm (d).

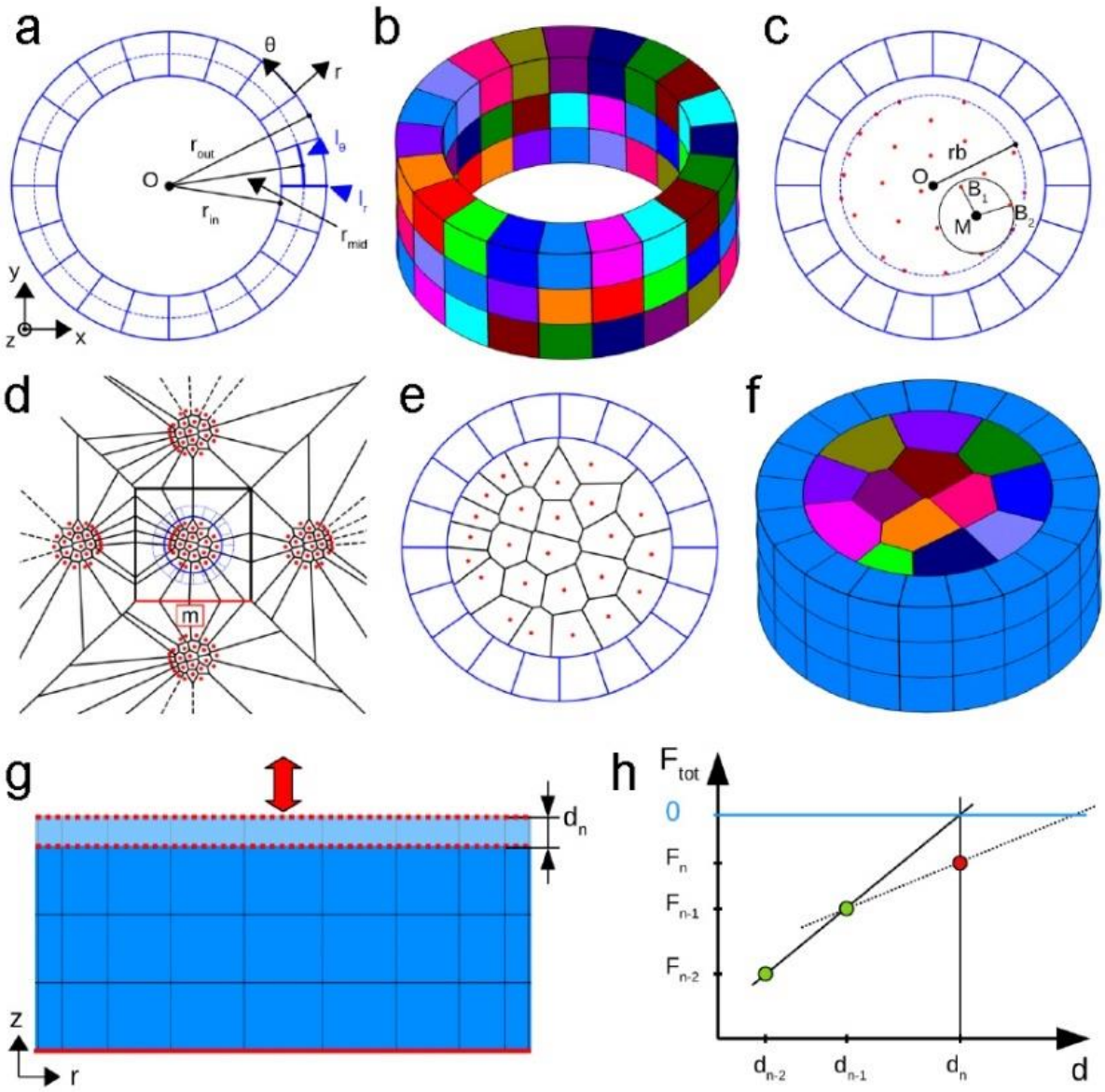

Extended Data Fig. 8. Cylindrical Voronoï construction and simulation. a, Construction of the cylindrical epidermis. **b**, 3D view of the cylindrical epidermis. **c,** 2D simplified schematic of the spring network used to place the Voronoï diagram control points within the epidermis. **d**, Symmetries of the cloud point and Voronoï diagram generation. **e**, Final Voronoï diagram. **f**, 3D view of a cylindrical Voronoï model. **g**, Side view of the model. Continuous red line indicates immobile vertices along the z axis. Dotted red line indicates the mobile plane that will adjust the axial force the model is subjected to. d_n is the current displacement of that plane. **h**, Estimation of the next displacement d_n based on the previous steps (d_{n-2}, F_{n-2}) and (d_{n-1}, F_{n-1}) shown as green dots and the goal force of 0 N. The new state (d_n, F_n) is represented as the red dot.

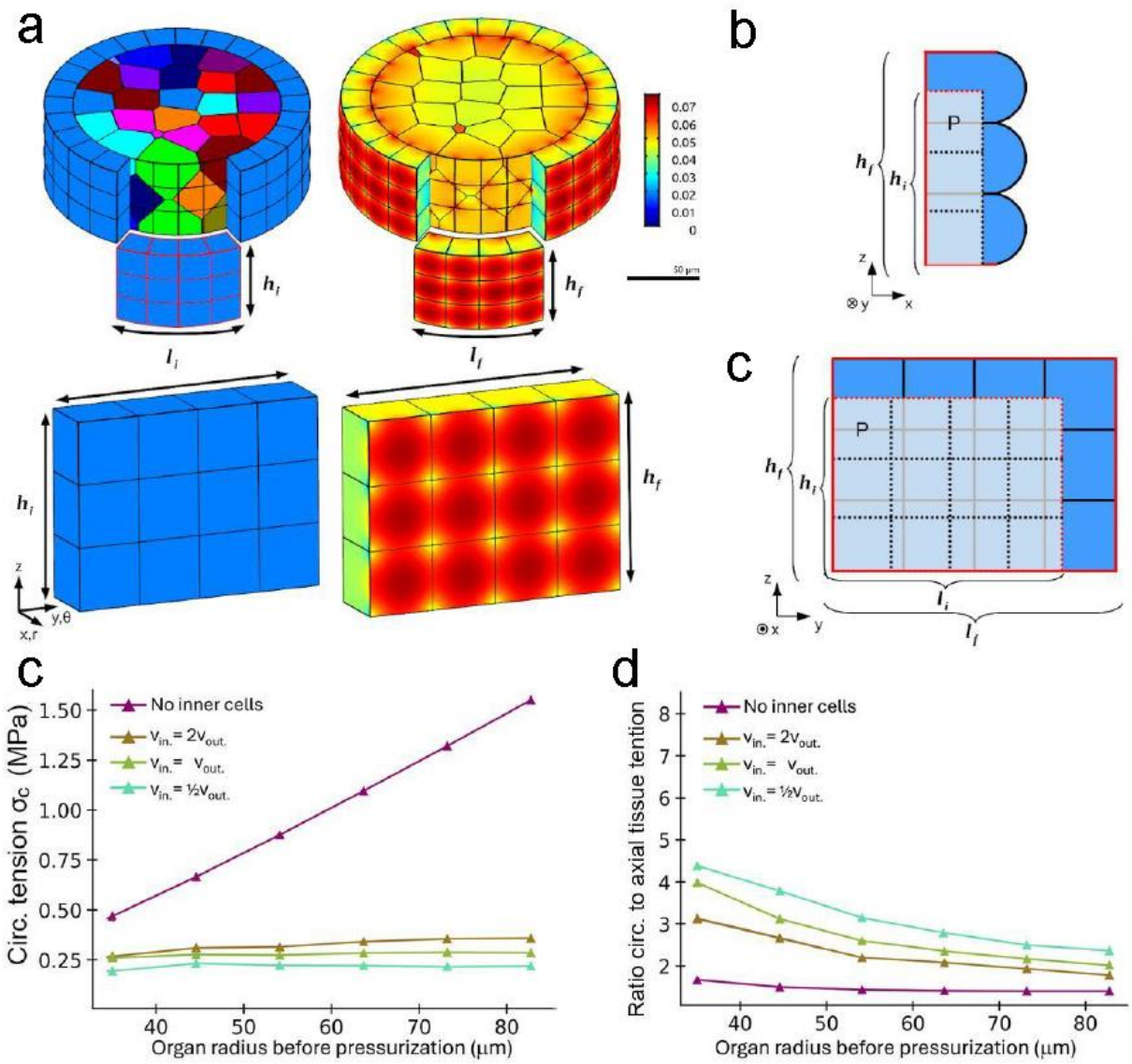

Extended Data Fig. 9 Construction of the flat twin model for the epidermis. a, Left side: Initial states of the voronoï in ring model and of the corresponding flat twin. Right side: Final states after pressurization. The color corresponds to the trace of the strain tensor. **b** and **c**, Superpositions of the initial and final simulation states of the flat twin model in the xz and yz planes respectively. The cell walls marked in red remain flat due to boundary conditions. The same walls in the yz plane are also moved to match the stretching of the epidermis. **d**, Tissue circumferential tension for varying inner over outer inflation potential ratios plotted against the organ radius before pressurization. **e**, Ratio of the tissue circumferential tension over the tissue vertical tension, plotted against the organ radius before pressurization.

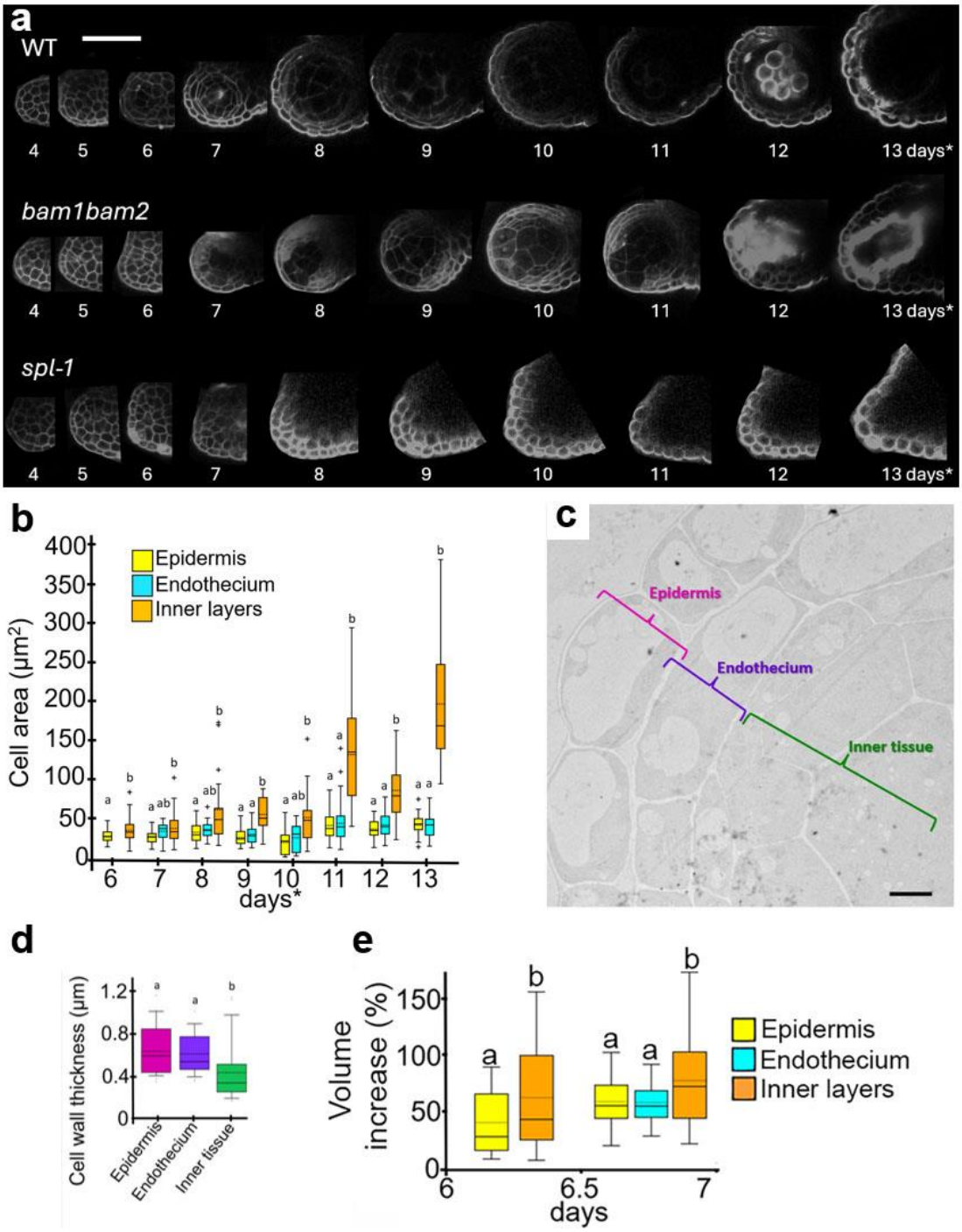

Extended Data Fig. 10 Emergence of endothecium reduces tension in the epidermis (a) Representative digital cross-sections of the anther lobe region in WT, *bam1bam2*, and *spl-1* from around 3 to 13 days*. Asterisk indicates estimated days after initiation. (**b**) Quantification of cell area per lobe region in WT anthers. For each time-point different letters indicate statistical significance, Mann-Whitney U test, $p<0.01$ ($n>10$ cells). Asterisk indicates estimated days after initiation. (**c**) Example of transmission electron microscopy micrograph of an anther lobe after "butterfly" shape acquisition. Brackets indicate the layers considered for measurements. (**d**) Quantification of cell wall thickness in different layers of the lobe. Different letters indicate statistical significance, Mann-Whitney U test, $p<0.01$ ($n>12$ cells). Asterisk indicates estimated days after initiation. (**e**) Different letters indicate statistical significance, Mann-Whitney U test, $p<0.01$. ($n>50$ cells, 4 time-lapse series). Scale bar, 40 µm (a) 2.5 µm. (b)